Numerical coupling of nonconservative or kinetic models with the conservative compressible Navier-Stokes equations

Jean-François Bourgat, Patrick Le Tallec, Moulay D. Tidriri, Youchun Qiu

INRIA

UNITÉ DE RECHERCHE
INRIA-ROCQUENCOURT

Institut National
de Recherche
en Informatique
et en Automatique

Domaine de Voluceau
Rocquencourt
B.P.105
78153 Le Chesnay Cedex
France
Tél. (1) 39 63 55 11

Rapports de Recherche

N° 1426

Programme 6
Calcul Scientifique, Modélisation et
Logiciels numériques

NUMERICAL COUPLING OF NONCONSERVATIVE OR KINETIC MODELS WITH THE CONSERVATIVE COMPRESSIBLE NAVIER-STOKES EQUATIONS

Jean-François BOURGAT
Patrick Le TALLEC
Driss TIDRIRI
Youchim QIU

Mai 1991

RR-1426

Numerical coupling of nonconservative or kinetic models with the conservative compressible Navier-Stokes equations.

Jean-François Bourgat, Patrick Le Tallec*, Driss Tidriri and Youchim Qiu

INRIA Rocquencourt, BP 105, 78153 Le Chesnay Cedex, France

Abstract : The purpose of this work is to couple different numerical models for the calculation of high speed external flows.
The proposed coupling is achieved by the boundary conditions, which impose viscous fluxes and friction forces on the body for the calculation of the global external flow and which impose Dirichlet type boundary conditions on the interface for the local model. *

=-=-=-=-=-=

Couplage numérique de modèles nonconservatifs ou cinétiques avec les équations de Navier-Stokes compressibles

---

Résumé : Le principe de ce travail consiste à coupler des modèles différents dans un calcul d'écoulements externes à grande vitesse. Le couplage proposé est imposé par le biais des conditions aux limites, qui imposent les forces de frottement et les flux de chaleur à la paroi pour le calcul Navier-Stokes et des conditions de Dirichlet pour le calcul du modèle local.

Mots-clés : Décomposition de domaines, couplage par frottement, Navier-Stokes, Boltzmann, hypersonique, gaz raréfiés.

---

* and Université de Paris Dauphine, 75775 Paris Cedex 16, France.
* INRIA Rocquencourt, BP 105, 78153 Le Chesnay Cedex, France.
This work was supported by the Hermes Research program under grant number RDAN 86.1/3.

1. Introduction

The purpose of this work is to couple different numerical models for the calculation of high speed external flows.

More precisely, we want to be able to introduce a specific treatment of the flow next to the body, this

i) for numerical purposes, in order to use locally a different solver (centered scheme,...) ;

ii) for approximation purposes, in order to use locally a much finer grid ;

iii) for physical motivations, in order to use locally a different equation such as non equilibrium chemical models or Boltzmann kinetic models.

The proposed coupling is achieved by the boundary conditions, which will impose viscous fluxes and friction forces on the body for the calculation of the global external flow and which will impose Dirichlet type boundary conditions on the local model.

2. Description of the coupling strategy

2.1. Navier-Stokes equations

Let us consider the compressible Navier-Stokes equations which we formally write either as

$$\frac{\partial W}{\partial t} + div[F(W)] = 0 \quad \text{on} \quad \Omega \text{ (conservative form)}$$

with $W = (\rho, \rho v, \rho E)$ and $U = (\rho, v, \theta)$ the conservative and non conservative variables, $F = F_C + F_D$ the total flux (convective and viscous part), T and D the convective and viscous terms in the nonconservative writing of the Navier-Stokes equations. The problem consists in computing a steady solution of these equations, with boundary conditions

$$\rho v, \rho E \text{ given on } \Gamma_\infty \text{ (exterior limit of the domain)},$$

$$\rho \text{ given on } \Gamma_\infty \cap \{x, v(x) \cdot n \leq 0\} \text{ (inflow)},$$

$$v = 0 \text{ on the body } \Gamma_o,$$

$$\theta = \theta_o \text{ on the body } \Gamma_o.$$

The global numerical treatment of these equations faces the following difficulties:
- in a conservative calculation, the numerical viscosity of the discretization scheme interferes with the physical viscosity and for a mesh of reasonable size leads to an overprediction of the boundary layer. Moreover, no slip boundary conditions on the body are difficult to handle for many TVD schemes ;
- in a nonconservative calculation, the correct calculation of a shock requires locally a very fine grid if we want to satisfy the Rankine Hugoniot conditions.

In this framework, our strategy will couple a *global conservative scheme*, defined on the whole domain, and based on a finite volume space discretization [1], and *a local approximation*, defined in the neighborhood of the body, which is presently based on a mixed Finite Element approximation of the nonconservative Navier-Stokes equations [2].

2.2. The Boltzmann equation

Denoting by $f(x,v,t)$ the distribution function of gas particles at time t, position x and with velocity v, the Boltzmann equation takes the form

$$\frac{\partial}{\partial t}f(x,v,t) + v \cdot \frac{\partial}{\partial x}f(x,v,t) = Q(f,f)(x,v,t)$$

with Q a collision operator, given by

$$Q(f,f)(x,v,t) = \int_{v_1}\int_{w\in S_2}(f_1'f' - ff_1)q(v-v_1,w)dwdv_1,$$

$$f_1 = f(x,v_1,t),$$

$$f' = f(x,v',t), v' = v + ((v_1 - v)\cdot w)w,$$

$$f_1' = f(x,v_1',t), v_1' = v_1 - ((v_1 - v)\cdot w)w.$$

Above $q(v-v_1,w)$ is the collision kernel ; for hard spheres, this kernel is proportional to $d^2|(v-v_1)\cdot w|$.

For rarefied gases, this equation must be used in place of the Navier-Stokes equations, especially in the immediate neighborhood of the body (Knudsen layer).

On the other hand, when density increases, collisions are very frequent, and the numerical treatment of the Boltzmann equations requires very fine grids, very long CPU time and is rapidly unfeasible.

Our strategy here will couple Navier-Stokes equations, used in their domain of validity far from the body and Boltzmann equations, to be used *locally* in a small domain next to the body. This strategy will then enable us to use more realistic kinetic boundary conditions on the body, avoiding the so-called slip boundary conditions generally used in such situations.

2.3. The general coupling strategy

For coupling global Navier-Stokes equations either with a local Navier-Stokes model, or with a local Boltzmann kinetic model, we introduce two domains, a global one Ω, a local one Ω_V included in Ω, and an interface Γ_i (Fig. 1). The global solution W on Ω and the local solution U_{loc} on Ω_V are matched by the following boundary conditions, inspired of Schwartz overlapping techniques :

$$\begin{cases} W = \text{ given imposed value on } \Gamma_\infty \\ n \cdot \sigma(W) \cdot \tau = n \cdot \sigma(U_{loc}) \cdot \tau \text{ on the body } \Gamma_o, \\ \text{(equality of friction forces)} \\ q(W) \cdot n + n \cdot \sigma(W) \cdot v = q(U_{loc}) \cdot n \quad \text{on} \quad \Gamma_o, \\ \text{(equality of total heat fluxes)} \\ v \cdot n = 0 \text{ on } \Gamma_o, \\ U_{loc} = 0 \text{ on } \Gamma_o \text{ (or an equivalent kinetic condition for the Boltzmann case)}, \\ U_{loc} = W \text{ on the interface} \Gamma_i. \end{cases}$$

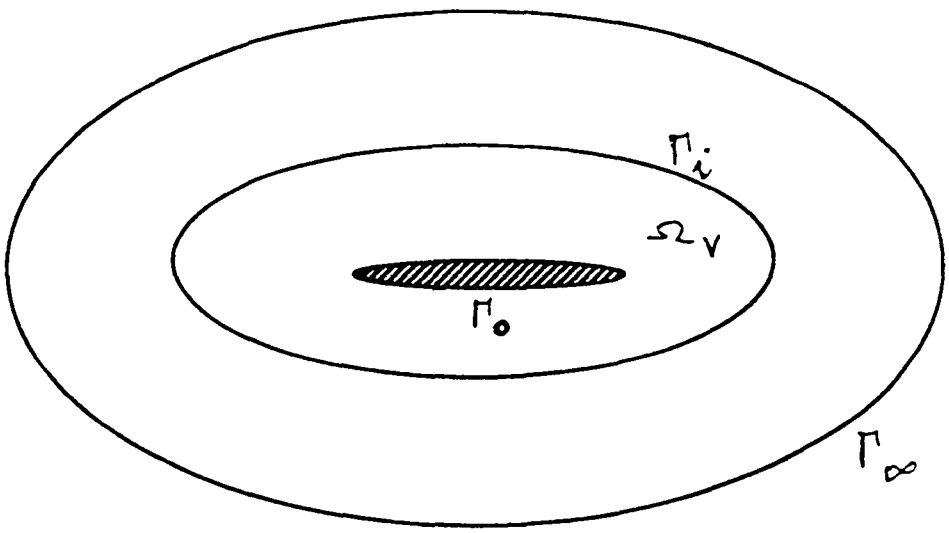

Fig. 1 : The global geometry

The calculation of U_{loc} and W satisfying the above boundary conditions is then obtained by a standard time marching technique, which leads to the following algorithm :

Initialization

1. Guess an initial distribution of the conservative variable W in the global domain Ω ;
2. Advance in time this distribution by using the global Navier-Stokes solver on N_1 time steps, with *Dirichlet* type boundary conditions on the body Γ_o ;
3. Deduce from this result an initial distribution of the local variable U_{loc} on the interface Γ_i and in the local domain Ω_V ;
4. Advance in time this distribution by using the local solver on N_2 time steps, with Dirichlet boundary conditions on Γ_i and Γ_o.

Iterations

5. From U_{loc}, compute the friction forces $n \cdot \sigma(U_{loc}) \cdot \tau$ and heat flux $q(U_{loc}) \cdot n$ on the body Γ_o ;
6. Advance the global solution in time (N_1 steps) by using the global Navier-Stokes solver, with the above viscous forces as boundary conditions on Γ_o (§2.4);
7. From W, compute the value of U_{loc} on the interface Γ_i ;
8. Using this new value as Dirichlet boundary conditions on Γ_i, advance the local solution in time (N_2 steps) and go back to step 5 until convergence is reached.

A parallel version of this algorithm is also quite possible although it is generally wiser to use parallel solvers within steps 6 and 8.

2.4. The global Navier-Stokes solver

The global domain Ω is discretized using node centered cells defined on an unstructured grid. Then, at each time step n and for each cell i, we solve

$$\int_{C_i} \frac{W^{n+1} - W^n}{\Delta t} + \sum_{j \in V(i)} \int_{\partial C_i \cap \partial C_j} F_C(W^{n+1}) \cdot n_i$$

$$+ \int_{\partial C_i - \Gamma} F_D(W^{n+1}) \cdot n_i + \int_{\partial C_i \cap \Gamma_\infty} F(W^{n+1}) \cdot n_i = - \int_{\partial C_i \cap \Gamma_o} F_o \cdot n_i.$$

In our numerical implementation, the fluxes F_C and F_D are computed at time step $n+1$ and linearized, with F_C computed by an Osher approximate Riemann solver [1]. The resulting linear system is solved by block relaxation.

On the body Γ_o, because of our special choice of boundary conditions, the flux is given by

$$\int_{\partial C_i \cap \Gamma_o} F_o \cdot n_i = \int_{\partial C_i \cap \Gamma_o} \begin{pmatrix} 0 \\ n_i \cdot \sigma(W^{n+1}) \cdot n_i \\ n_i \cdot \sigma(U_{loc}) \cdot \tau_i \\ q(U_{loc}) \cdot n_i \end{pmatrix},$$

where the aspect of a boundary cell C_i is described in Fig. 2.

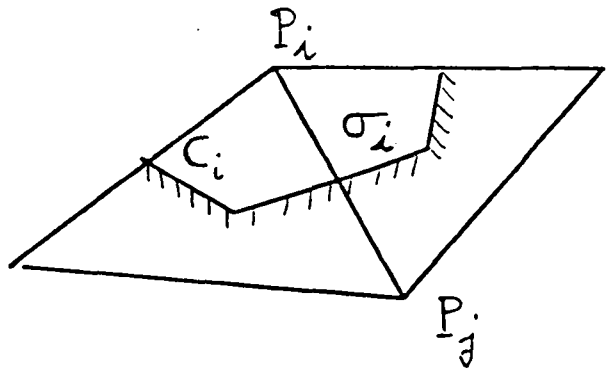

Fig. 2 : A boundary cell

In other words, friction forces and heat flux are given explicitly by the local solver and the mass flux is imposed to zero. Then, in order to have a well-posed problem (at least in the incompressible case [4]), the normal stress (the multiplier of the zero mass flux constraint) cannot be imposed and must be obtained from the solution W^{n+1}.

Remark : Imposing friction forces to the global solution instead of no slip boundary conditions allows to have an accurate solution away from the boundary layer even with a coarse mesh (§2.6 [5]).

3. Coupling conservative and nonconservative schemes

3.1. The local solver

In this case, the local solver takes the form

. let $U^o = (\rho, v, \theta)$ be computed at the previous call of the local solver ;

. let $U_i = (\rho, v, \theta)$ on Γ_i be computed by interpolation from the values of the global solution W on the interface ;

. for $n = 0$ to N_2, solve the local nonconservative Navier-Stokes equation

$$\begin{cases} \displaystyle\int_{\Omega_V} \frac{U^{n+1} - U^n}{\Delta t} \cdot \hat{U}_j + \int_{\Omega_V} (T + D)(U^{n+1}) \cdot \nabla \hat{U}_j = 0, \forall j \\ U^{n+1} = U_i \quad \text{on} \quad \Gamma_i, \\ (v^{n+1}, \theta^{n+1}) = (0, \theta_o) \quad \text{on} \quad \Gamma_o. \end{cases}$$

Here the nonconservative Navier-Stokes equations are discretized by mixed Finite Elements (P_1 for ρ and θ, P_1 on the subdivided P_2 grid for the velocity). The test functions $\hat{U}_j$ correspond then to the shape functions of the corresponding Finite Element spaces. The resulting nonlinear system is solved by a few steps of a nonlinear GMRES solver with diagonal preconditioning.

In output, friction forces and heat flux are given by

$$\sigma(U_{loc}) = \mu(\theta^{n+1})((\nabla v^{n+1} + \nabla^t v^{n+1})/2 - \frac{1}{3} div v^{n+1} Id),$$

$$q(U_{loc}) = \lambda \frac{\partial \theta^{n+1}}{\partial n}.$$

Remark

i) The Dirichlet condition on Γ_i can be replaced by a Neumann type boundary condition of the type

$$(T + D)(U^{n+1}) = g(W) \quad \text{on} \quad \Gamma_i.$$

Such a condition might lead to an easier local problem, since it does not impose a fixed value of the density on an outflow boundary.

ii) The nonconservative approach simplifies the calculation of the viscous terms and is well suited to flows at low Mach numbers. On the other hand, it cannot treat hypersonic situations. There, the local solvers must also be conservative.

3.2. The numerical test

The test problem considers a two dimensional flow around an ellipse, with 0 angle of attack, $M_\infty = 0.85$, Reynolds number = 100, and a wall temperature $T_W = 2.82 T_\infty$.

Four different numerical solutions have been computed.

i) The first one uses the global solver with no slip boundary conditions on a "coarse" mesh having 4033 nodes and 7942 elements.

ii) The second one uses the same solver with the same boundary conditions but on a finer mesh having 16008 nodes and 31768 elements. This will be our reference solution.

iii) The third one uses the local nonconservative solver to solve the problem on the whole domain Ω. Its velocity mesh is identical to the mesh used in (ii).

iv) The last one uses the coupling strategy of §2 ; the global solver uses the coarse mesh of case (i), the local solver uses the restriction to Ω_V of the mesh of case (iii) ("fine" grid for velocity, "coarse" grid for density and temperature).

The reference numerical results are shown on Figure 3 (Mach contours), 4 (skin friction coefficient C_f on the body), 5 (heat flux coefficient $S_n = \frac{2\gamma}{Re Pr} \frac{\partial \theta}{\partial n}$), 6 (local mesh) and 7 (velocity field in the wake). We observe small vortices in the wake, which can only be detected by a fine mesh, and large viscous effects.

Compared to this reference calculation, the coarse mesh calculation of case (i) gives the same Mach contours, but the maximum C_f is now 0.35 (instead of 0.40) and the maximum S_n is 0.084 (instead of 0.062).

As for the global nonconservative calculation (iii) and the coupled calculation (iv), they are both perfect for the Mach contours and for C_f (less than 3% error), but overshoot the maximum value for S_n (0.085).

This indicates that the temperature grid (which is the coarse grid of (i)) is too coarse. If we now decrease the size of the computational domain to less than twenty times the length of the body, the global nonconservative calculation is very rapidly polluted, which is not the case for the coupled problem.

A last output of the coupled approach is the value of the tangential velocity computed on the body by the global solver (Fig. 8). This value is very small

which means that the global mesh is reliable. When the mesh gets too coarse, the C_f are correctly predicted by a coupled approach and not by a global one with Dirichlet boundary conditions. In other words, the coupled approach gives both an error estimate and a protection against coarse meshes.

In summary, for sufficiently fine meshes, all three numerical approaches (global conservative, global nonconservative and coupled) give good results. Compared to the global nonconservative approach, the coupled approach is more robust and can use much smaller computational domains. Compared to the global conservative approach, the coupled method requires fine grids in much smaller regions and allows a large flexibility in the definition of boundary conditions. This flexibility will even be larger in the Boltzmann case of §4.

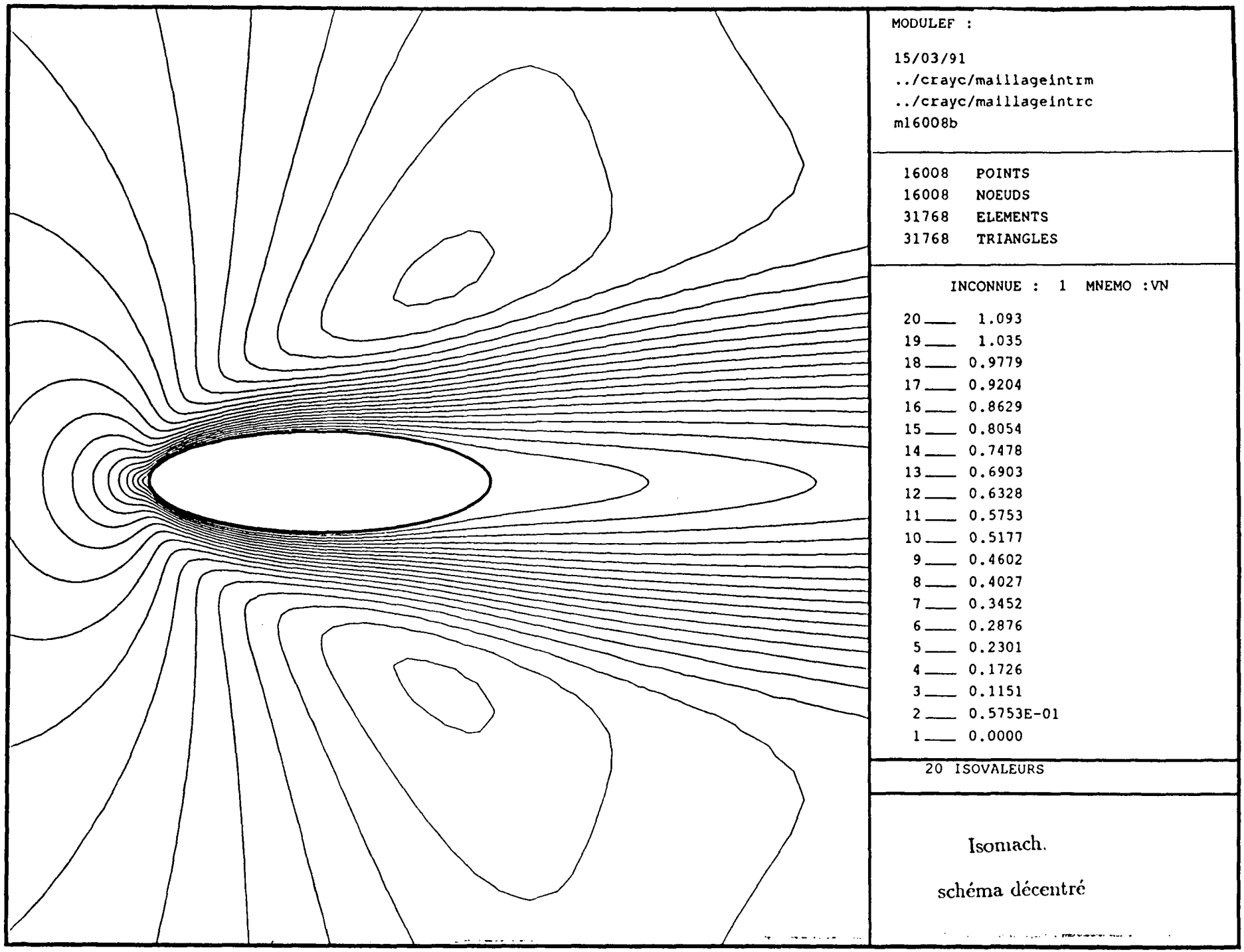
MODULEF :
15/03/91
../crayc/maillageintrm
../crayc/maillageintrc
m16008b
16008 POINTS
16008 NOEUDS
31768 ELEMENTS
31768 TRIANGLES
INCONNUE : 1 MNEMO :VN
20 1.093
19 1.035
18 0.9779
17 0.9204
16 0.8629
15 0.8054
14 0.7478
13 0.6903
12 0.6328
11 0.5753
10 0.5177
9 0.4602
8 0.4027
7 0.3452
6 0.2876
5 0.2301
4 0.1726
3 0.1151
2 0.5753E-01
1 0.0000
20 ISOVALEURS
Isomach.
schéma décentré

Fig. 3

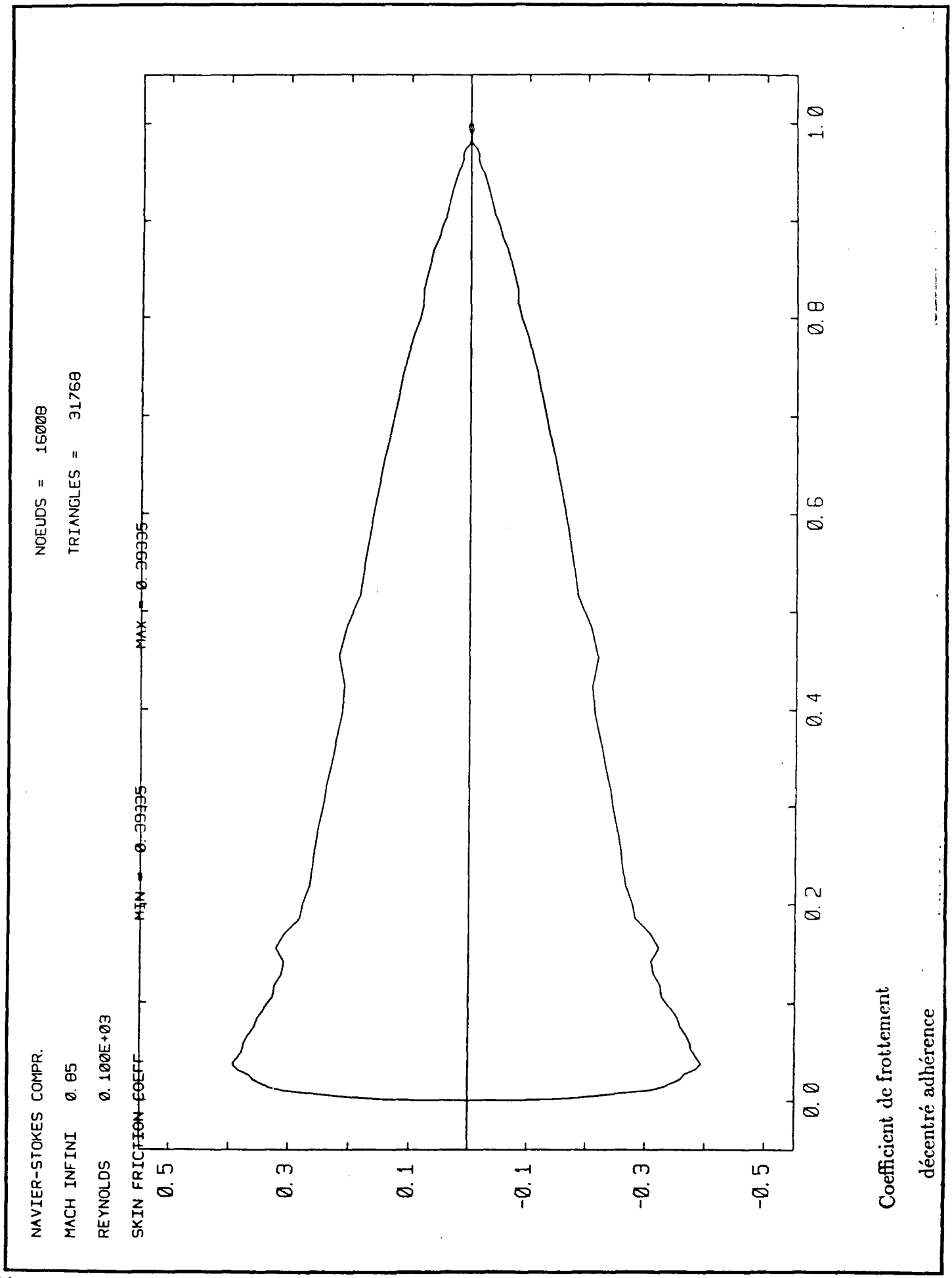
NAVIER-STOKES COMPR.
MACH INFINI 0.85
REYNOLDS 0.100E+03
NOEUDS = 16000
TRIANGLES = 31768
SKIN FRICTION COEFF MIN = -0.39335 MAX = 0.39335
0.5
0.3
0.1
-0.1
-0.3
-0.5
0.0
0.2
0.4
0.6
0.8
1.0
Coefficient de frottement
décentré adhérence

Fig. 4

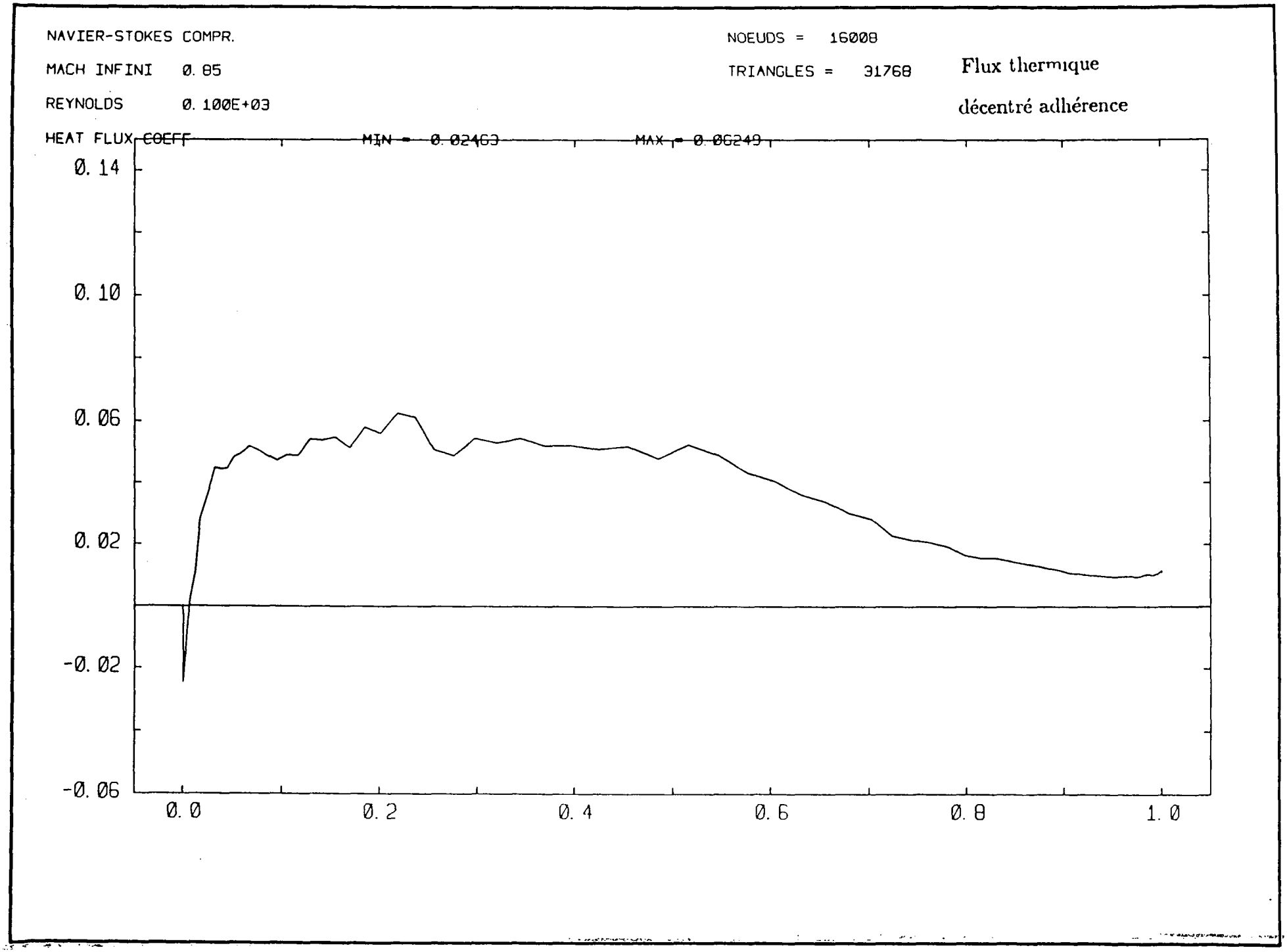

Flux thermique

décentré adhérence

Fig. 5

MODULEF
18/03/91
maillageintrm
maillageintrc
16008 POINTS
16008 NOEUDS
31768 ELEMENTS
31768 TRIANGLES
Loupe maillage fin

Fig. 6

MODULEF
18/03/91
maillageintrm
maillageintrc
../cray1/v16008b
16008 POINTS
16008 NOEUDS
31768 ELEMENTS
31768 TRIANGLES
EXTREMA DU CHAMP B :
0.00 1.2
ECHELLE :
50. CM. = 1.2
Champs de vitesse
VITESSES

Fig. 7

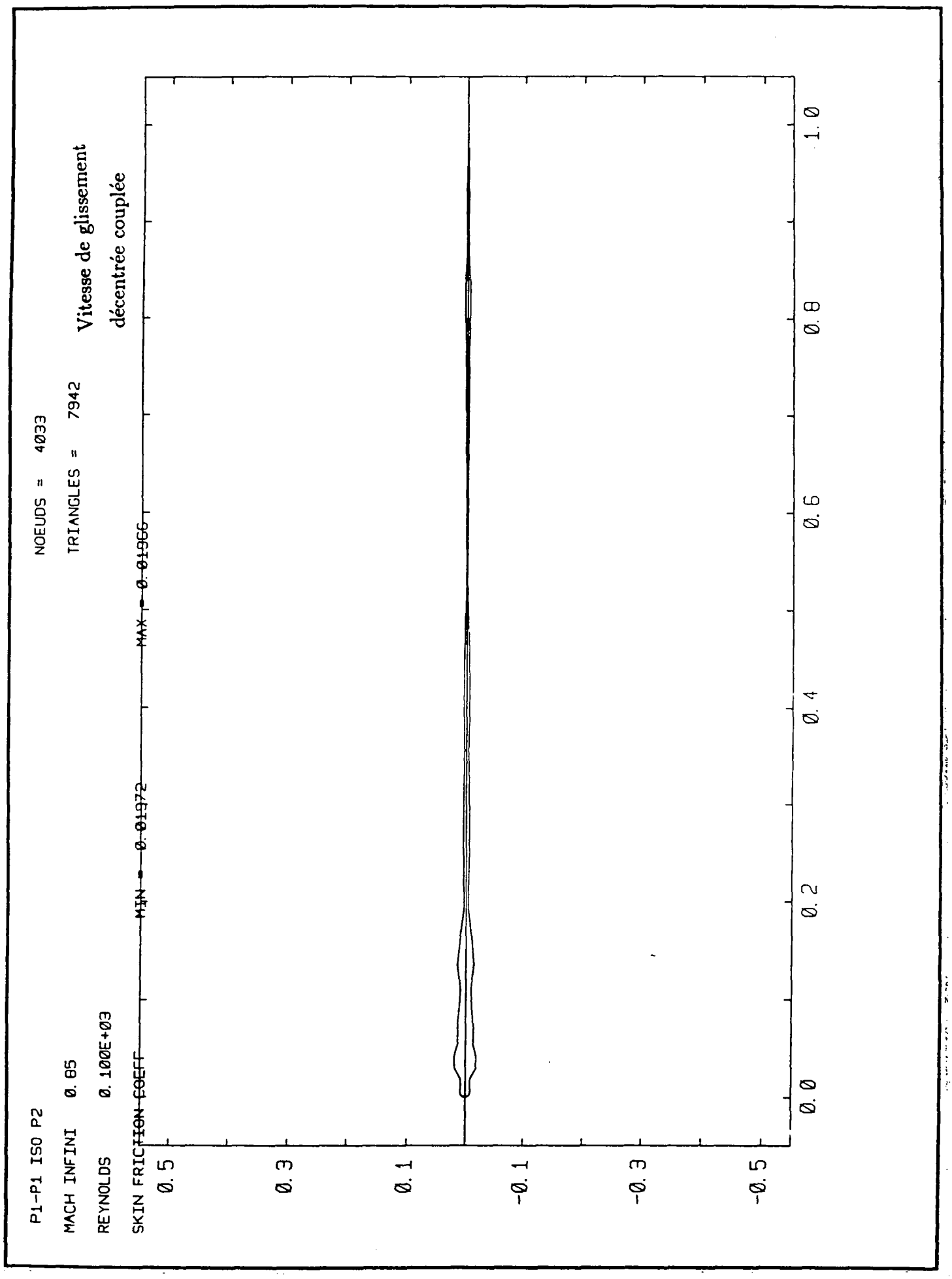
P1-P1 ISO P2
MACH INFINI 0.85
REYNOLDS 0.100E+03
SKIN FRICTION COEFF MIN = 0.01972 MAX = 0.01966
NOEUDS = 4033
TRIANGLES = 7942
Vitesse de glissement
décentrée couplée
0.5
0.3
0.1
-0.1
-0.3
-0.5
0.0
0.2
0.4
0.6
0.8
1.0

Fig. 8

3.3. Convergence properties

As described in [5], numerical tests run for a linear advection diffusion problem show that the coupling algorithm is linearly convergent when Δt is below a limit value which increases with the Reynolds number. A one dimensional analysis shows that this condition is necessary, an asymptotic analysis done for Δt and h small ([4]) shows that such a condition is sufficient.

There were no convergence problems in the numerical tests of §3.2. For cases (i) and (ii), using local time steps, we reach a residual value of 10^{-12} after 1650 iterations in case (i) and 6270 iterations in case (ii), the residual being given by

$$r_d = \frac{\|(\rho^{n+1} - \rho^n)/\Delta t^n\|_{0,2}}{\|(\rho^1 - \rho^o)/\Delta t^o\|_{0,2}}.$$

For the global nonconservative calculation of (iii), we reach a residual value of $0.4\ 10^{-7}$ after 900 iterations with

$$r_c = \|\frac{\partial \rho}{\partial t}\|_{0,2}/mes(\Omega).$$

For the coupled approach, run with $N_1 = 450$ and $N_2 = 50$ in the initialization process, and with $N_1 = N_2 = 1$ in the iterations, we reach a residual value of 10^{-3} after 50 iterations.

4. The Boltzmann/Navier-Stokes coupling

4.1. The local solver

In this case, the local solver is a Monte Carlo method developed at the University of Kaiserslautern, and corresponds to the following algorithm :

- Define an initial particle distribution (§4.2) ;
- Loop on time. For each time step :

1. generate particles at the interface Γ_i (§4.3),
2. advance the particles by free transport : $x_i^{n+1} = x_i^n + v_i^n \Delta t$,
3. erase the particles which have left the computational domain through Γ_i,
4. treat the particles which have collided with the body (§4.4),
5. regroup particles together in small cells,
6. in each cell, make the different particles collide by coupling them randomly and randomly picking the corresponding collision parameters ([3]).

In output, the average values ρ, u, T and the wall fluxes are obtained by averaging on all cell particles j and on several ($N \simeq 100$) consecutive time steps:

$$\rho = \frac{1}{N \cdot Vol\ Cell} \sum_n \sum_j m_j$$

$$u = \frac{1}{\rho \cdot N \cdot Vol\ Cell} \sum_{n,j} m_j v_j,$$

$$\frac{3}{2}RT = \frac{1}{\rho \cdot N \cdot Vol\ Cell} \sum_{n,j} \frac{1}{2} m_j v_j^2 - \frac{1}{2} v^2.$$

4.2. Constructing a particle distribution

In order to minimize storage requirements, the particle distribution is not stored between two calls of the Boltzmann solver. We just store the average values ρ, u and T for each cell i. Then, at each Boltzmann step, we construct the initial particle distribution on cell i by randomly distributing $\rho_i \frac{N_{ref}}{\rho_{ref}}$ particles on the cell i, distributing velocities with the Maxwell probability law

$$M(v) = \frac{\rho_i}{(2\Pi RT_i)^{\frac{3}{2}}} exp(-(v-u_i)^2/2RT_i).$$

4.3. Generating particles on the interface

In our coupling strategy, the values of the local solution on the interface Γ_i must be obtained from the values of the global Navier-Stokes solution W on this interface. For Boltzmann, this is simply achieved by defining a layer of cells around the local domain Ω_V (Fig. 9). Then we define the average values ρ, u and T in these cells by interpolating the values of the global solution W at the cell center. Finally, from ρ, u and T, we construct a particle distribution on these cells as done in §4.2, and proceed with the other steps of the local solver.

This particle construction is done at each time step.

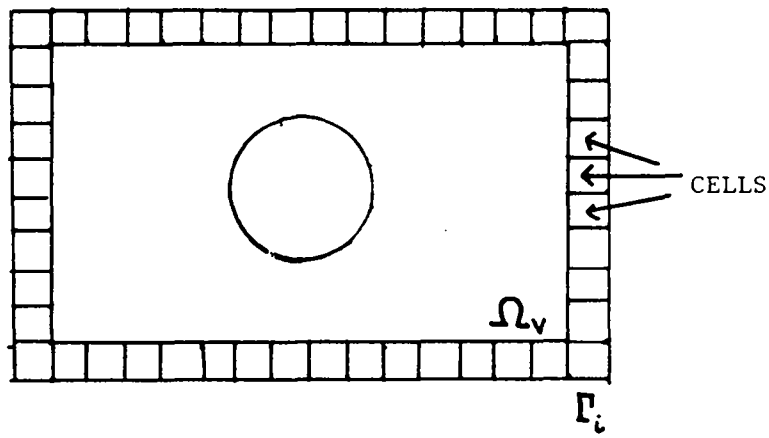

Fig. 9 : Interface between Boltzmann and Navier-Stokes

4.4. Wall boundary conditions

In kinetic theory, the interaction of gas molecules with the body surface is modelled by a boundary condition on the distribution $f(x,v,t)$. Between all possible models, the most popular is the so-called accomodation model in which every particle which collides with the wall is reemitted with a random velocity whose distribution obeys a Maxwell law at wall temperature T_W. At the numerical level, for each particle colliding with the wall, we pick four random numbers a_i in the intervall $(0,1)$ and define its output velocity in an accomodation model by

$$v_n = \sqrt{-T_W log a_4}\, cos 2\Pi a_2,$$

$$v_\tau = \sqrt{-T_W log\, a_3}(cos 2\Pi a_1 e_x + sin 2\Pi a_1 e_y).$$

Here v_n is the velocity normal to the wall, e_x and e_y are two orthonormal vectors tangent to the wall and v_τ is the particle tangential velocity.

4.5. Computing fluxes at the wall

These fluxes are computed from their kinetic definition. Under the notation
n = unit normal vector, exterior to the flow field,
Γ = portion of body surface where fluxes are computed,
dS = area of Γ,
dt = considered time interval,
J = set of particles colliding with Γ during time interval dt,

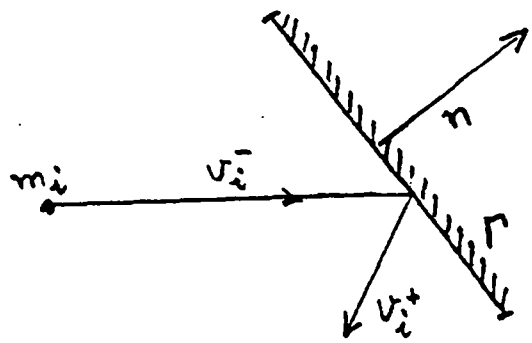

Fig. 10

the quantity $\sigma \cdot ndSdt$ is equal to the sum of all impulses received by particles which collide with Γ during the time interval dt, that is

$$\sigma \cdot ndSdt = \sum_{i \in J} m_i (v_i^+ - v_i^-).$$

Similarly, the total flux $q \cdot ndSdt$ is the energy given by the particles to the wall during collision, that is

$$q \cdot ndSdt = -\sum_{i \in J} \frac{1}{2} m_i (|v_i^+|^2 - |v_i^-|^2).$$

4.6. Numerical test

On the same ellipse as before, we compute a rarefied flow corresponding to $M_\infty = 5$ and Reynolds number = 300.
More precisely, we have

$$\begin{cases} T_\infty = 194^o, \\ T_W = 1000^o, \\ \text{Mean Free path} = 0.1977m, \\ \text{Ellipse length} = 7m. \end{cases}$$

This case is computed by four different physical models. For each case, we present the Mach contours (Fig. 11) and the friction coefficient (Fig. 12).

Case 1 : Navier-Stokes with no slip boundary conditions ($\gamma = 1.414$)

The mesh contains 2247 nodes and 4374 elements. The numerical solution is rather easy to compute, but in the rear part of the body the density is low and the friction coefficient high, which is not very physical.

Case 2 : Navier-Stokes with slip boundary conditions ($\gamma = 1.414$)

The boundary conditions on the body are here ([6])

$$\begin{cases} u \cdot n = 0, \\ n \cdot \dfrac{\nabla u + \nabla^t u}{2} \cdot \tau = -A\rho u \cdot \tau. \end{cases}$$

These boundary conditions which are popular in rarefied flows computations, are very difficult to handle ; even with a mesh of 5544 nodes and 10888 elements, we could not avoid a singularity of the friction coefficient in the rear part of the body (Fig. 12.2, with $\rho_\infty = 10^{-6} kg/m^3$ and $A = 7.92$). Actually, the above boundary conditions which are derived for a rarefied boundary layer are completely unjustified in this flow situation.

Case 3 : Boltzmann with accomodation($\gamma = 1.2$)

The mesh here contains 5985 cells with 25 particles per cell. The collision kernel corresponds to the hard spheres model.

Case 4 : Coupled model (local Boltzmann model with $\gamma = 1.2$, global Navier-Stokes model with $\gamma = 1.414$)

This first coupled model is inconsistent from the physical point of view (γ is different in Navier-Stokes and in Boltzmann) but it was run for qualitative purposes. There were 4 coupling iterations with $N_1 = N_2 = 100$. At this stage, the interface values have reached their asymptotic limit, and the coupling algorithm can be safely stopped. In the initialization process, the global solver was used for 300 iterations ($CFL = 5$) with no slip boundary conditions.

The corresponding results are compatible with those of a Boltzmann simulation. A rarefied region appears in the wake (Fig. 11.4, 11.5) and the friction coefficients are smoothly decreasing in the rear part of the body (Fig. 12.4). The same behavior can be observed on the Stanton number. As for the tangential velocity on the body as predicted by the coupled global Navier-Stokes solver, it is non zero but smaller than the one predicted by the slip model of case 2.

4.7. Conclusion

The preceding test is based on a coupling strategy which on one hand bypasses the problem of getting adequate boundary conditions for rarefied flows Navier-Stokes solutions and on the other hand reduces the computational domain of the Boltzmann simulation. This test :

i) proves the feasibility of the coupling approach,

ii) leads to a reasonable solution,

iii) illustrates the weakness of the Navier-Stokes approach in such situations.

This test must be completed by a more systematic analysis of rarefied flows and by using more sophisticated kinetic models for collisions and boundary conditions.

References

[1] Ph. Rostand, B. Stoufflet : Finite volume Galerkin methods for viscous gas dynamics. Rapport de recherche INRIA no 863, Juillet 1988.

[2] M.O. Bristeau, R. Glowinski, L. Dutto, J. Périaux, G. Rogé : Compressible viscous flow calculations using compatible finite element approximations ; 7th Int. Conf. on Finite Element Methods in Flow Problems, Huntsville, Alabama (1989) ; et International Journal for Numerical Methods in Fluids 11 (1990), pp. 719-749.

[3] C. Cercignani : Theory and Applications of the Boltzmann equation, Scottish Academic Press, (1975).

[4] M. Tidriri, Thèse, en préparation.

[5] P. Le Tallec, M. Tidriri, Couplage et conditions aux limites, Rapport de contrat, Juillet 1990.

[6] Ph. Rostand, Thèse, Université Paris VI, (1989).

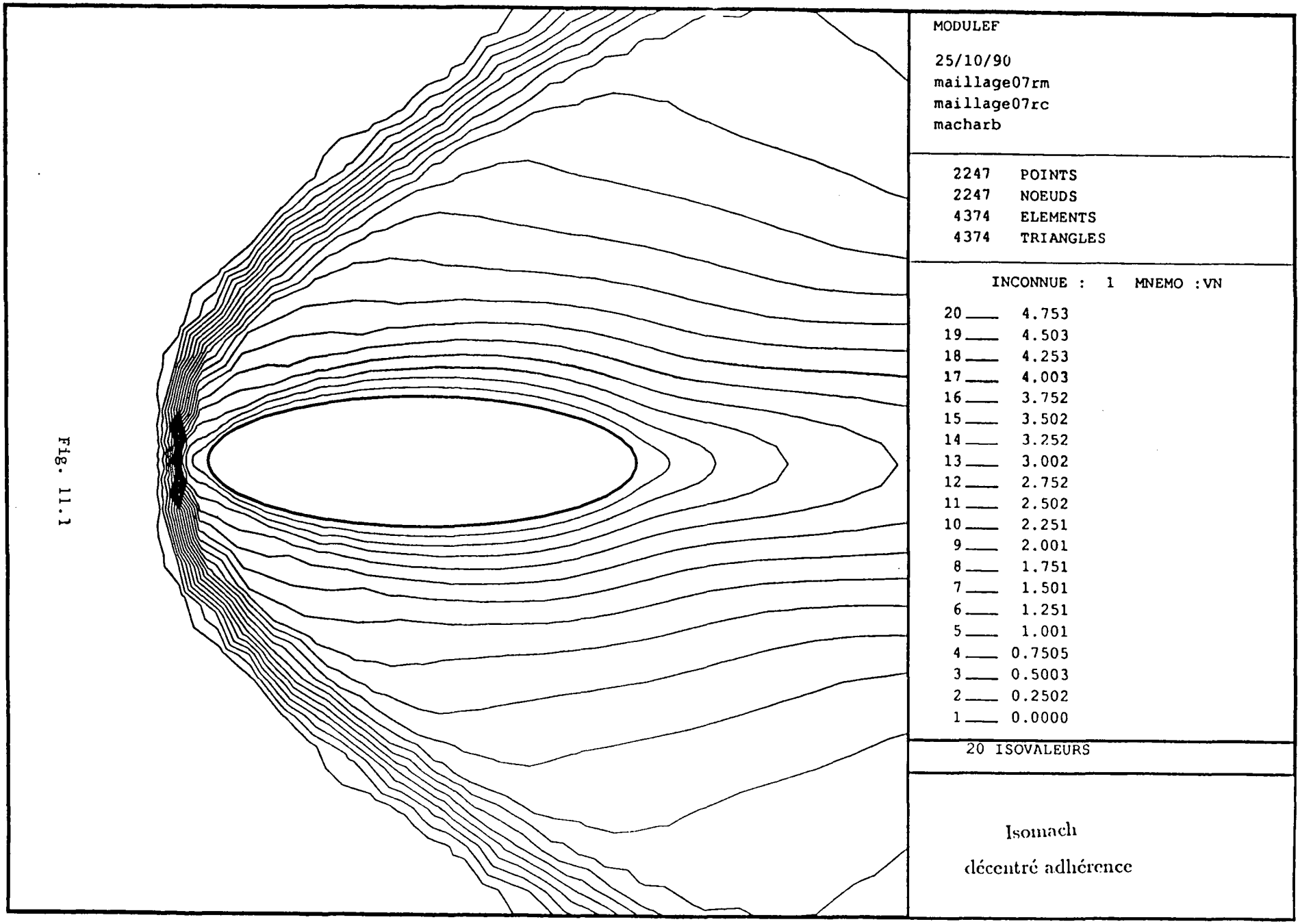
MODULEF
25/10/90
maillage07rm
maillage07rc
macharb
2247 POINTS
2247 NOEUDS
4374 ELEMENTS
4374 TRIANGLES
INCONNUE : 1 MNEMO :VN
20 4.753
19 4.503
18 4.253
17 4.003
16 3.752
15 3.502
14 3.252
13 3.002
12 2.752
11 2.502
10 2.251
9 2.001
8 1.751
7 1.501
6 1.251
5 1.001
4 0.7505
3 0.5003
2 0.2502
1 0.0000
20 ISOVALEURS
Isomach
décentré adhérence

Fig. 11.1

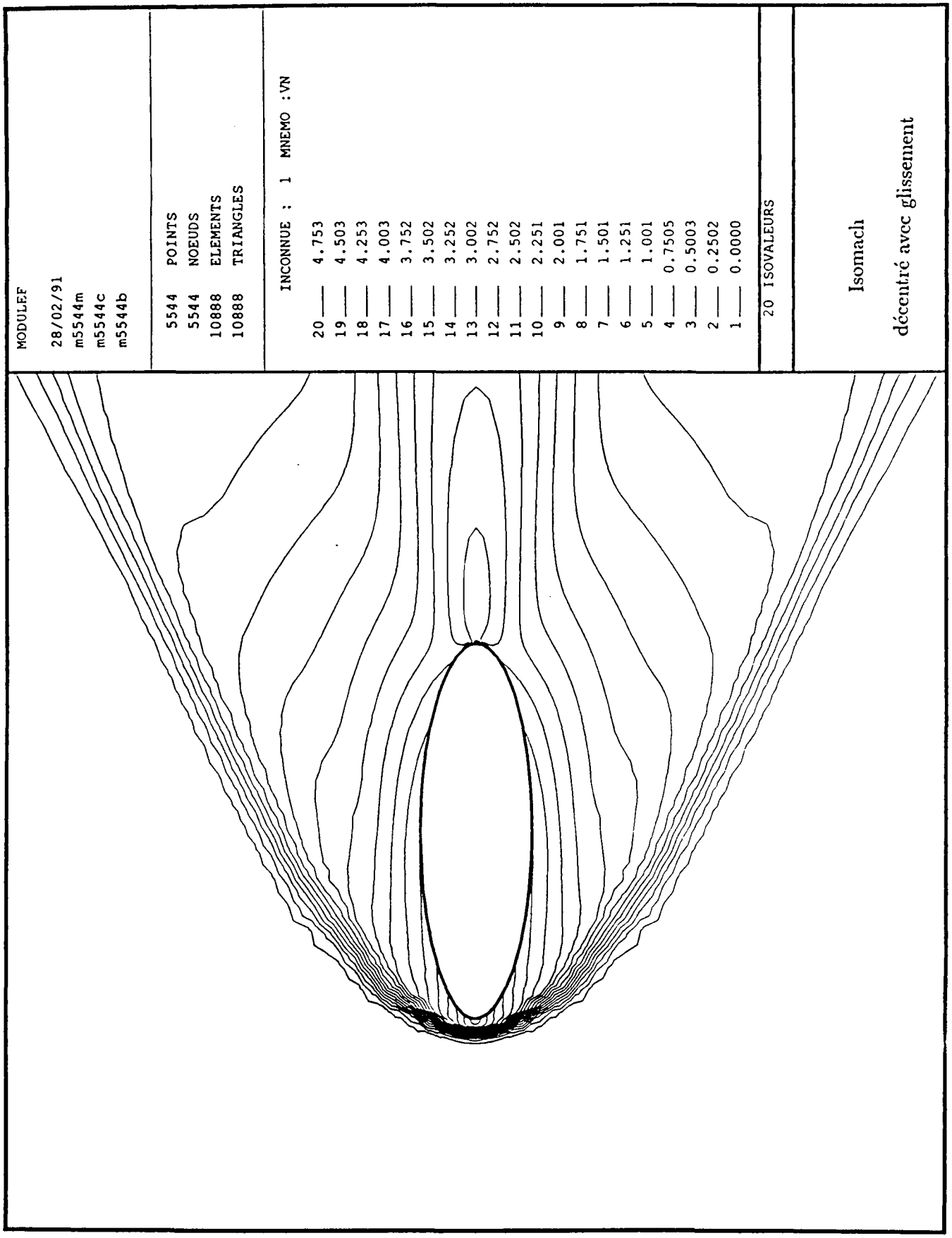
MODULEF
28/02/91
m5544m
m5544c
m5544b
5544 POINTS
5544 NOEUDS
10888 ELEMENTS
10888 TRIANGLES
INCONNUE : 1 MNEMO :VN
20 4.753
19 4.503
18 4.253
17 4.003
16 3.752
15 3.502
14 3.252
13 3.002
12 2.752
11 2.502
10 2.251
9 2.001
8 1.751
7 1.501
6 1.251
5 1.001
4 0.7505
3 0.5003
2 0.2502
1 0.0000
20 ISOVALEURS
Isomach
décentré avec glissement

Fig. 11.2

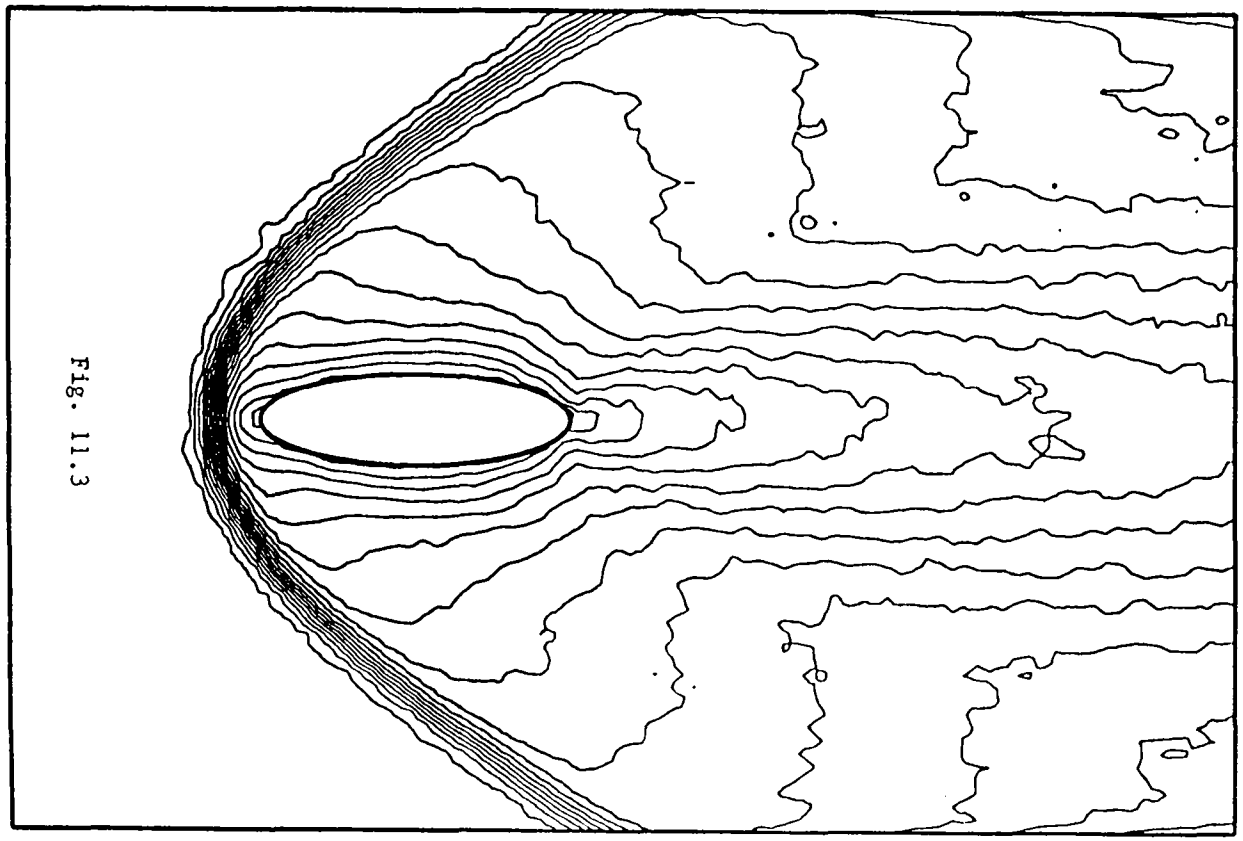

Fig. 11.3

MODULEF
Mach
14/12/90
mail
coor
m

6144 POINTS
6144 NOEUDS
5985 ELEMENTS
5985 QUADRANGLES

INCONNUE : 1 MNEMO :VN

20 ___ 4.707
19 ___ 4.460
18 ___ 4.212
17 ___ 3.964
16 ___ 3.716
15 ___ 3.469
14 ___ 3.221
13 ___ 2.973
12 ___ 2.725
11 ___ 2.478
10 ___ 2.230
9 ___ 1.982
8 ___ 1.734
7 ___ 1.487
6 ___ 1.239
5 ___ 0.9910
4 ___ 0.7433
3 ___ 0.4955
2 ___ 0.2478
1 ___ 0.0000

20 ISOVALEURS

Isomach

Boltzmann sur domaine global

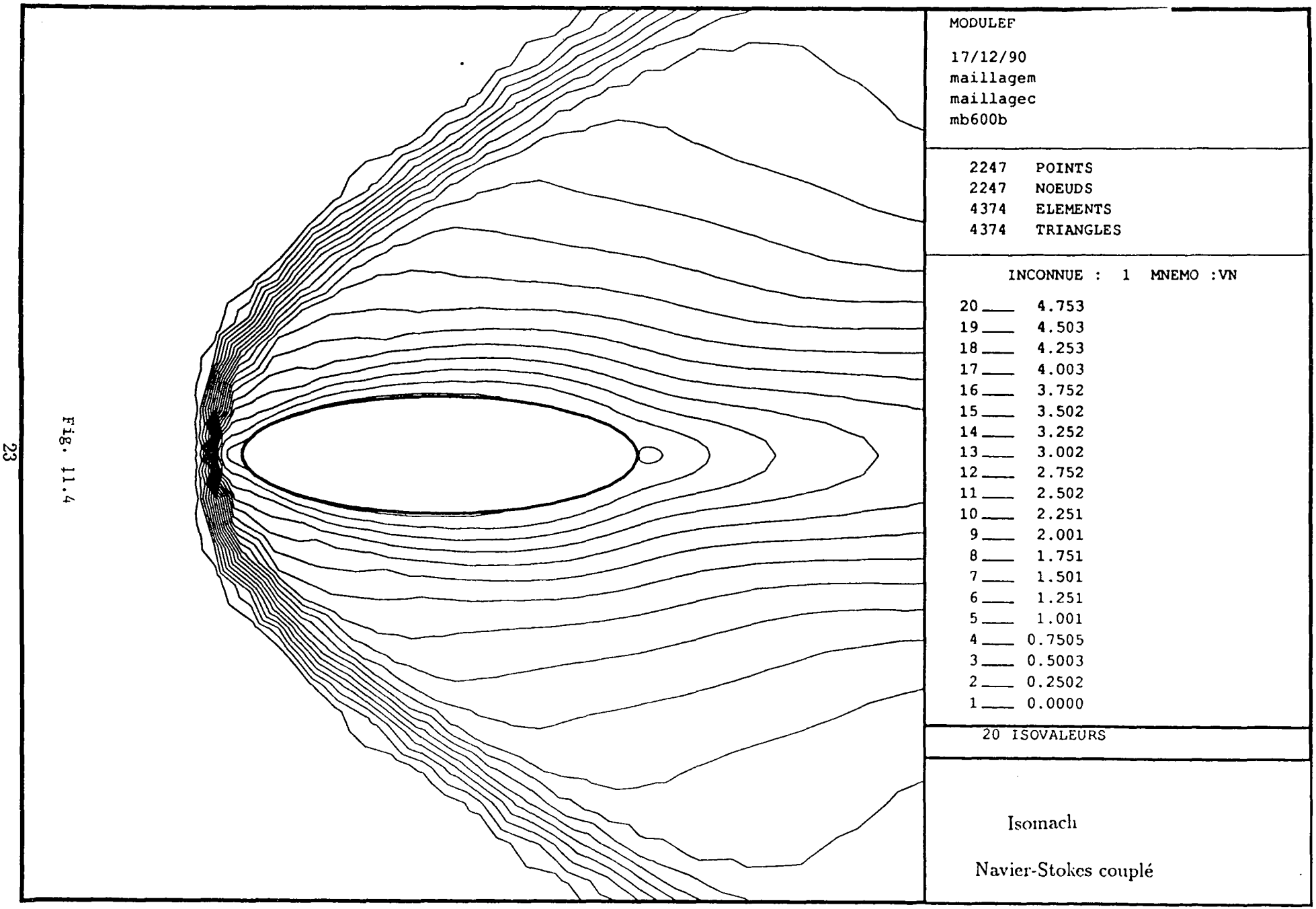
MODULEF
17/12/90
maillagem
maillagec
mb600b
2247 POINTS
2247 NOEUDS
4374 ELEMENTS
4374 TRIANGLES
INCONNUE : 1 MNEMO :VN
20 4.753
19 4.503
18 4.253
17 4.003
16 3.752
15 3.502
14 3.252
13 3.002
12 2.752
11 2.502
10 2.251
9 2.001
8 1.751
7 1.501
6 1.251
5 1.001
4 0.7505
3 0.5003
2 0.2502
1 0.0000
20 ISOVALEURS
Isomach
Navier-Stokes couplé

Fig. 11.4

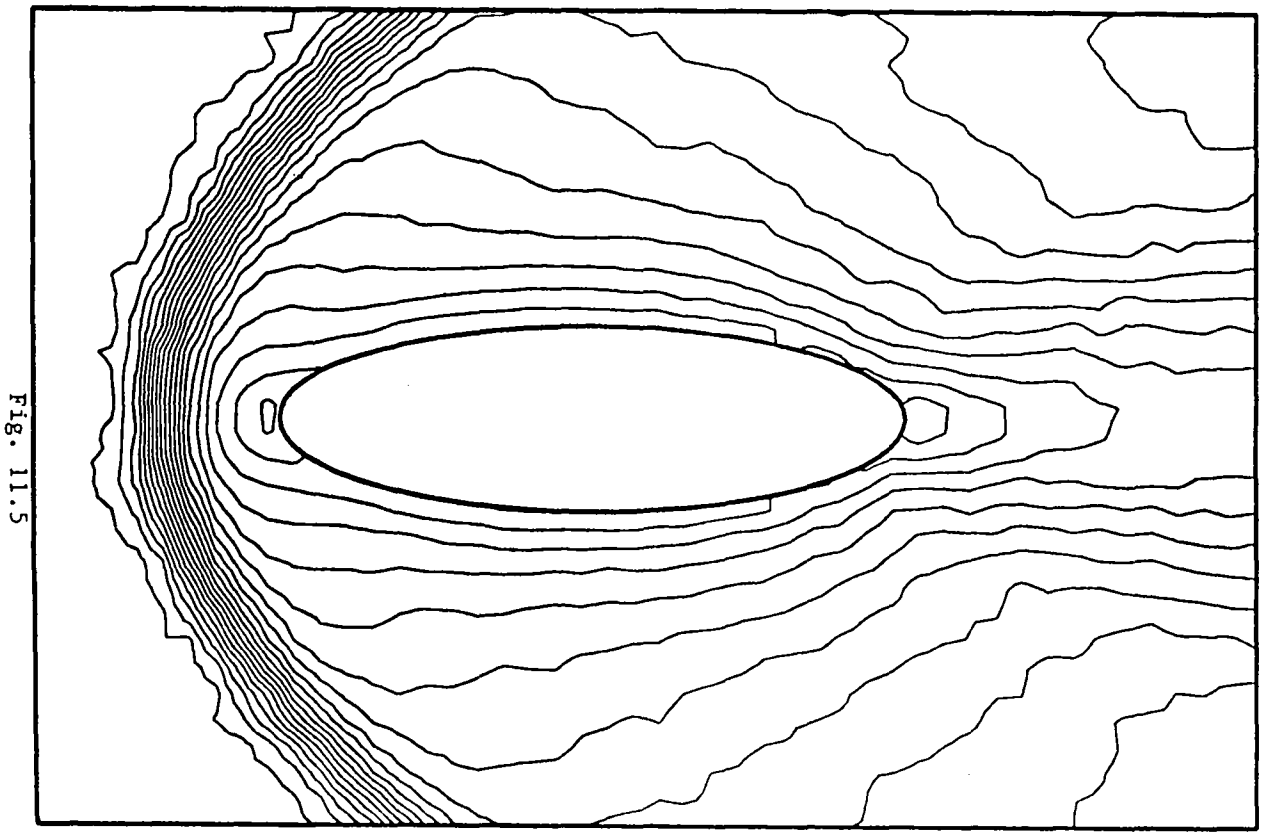

Fig. 11.5

MODULEF
mach(4i
21/12/90
mail
coor
m4

1536 POINTS
1536 NOEUDS
1457 ELEMENTS
1457 QUADRANGLES

INCONNUE : 1 MNEMO :VN

20	4.500
19	4.276
18	4.053
17	3.829
16	3.605
15	3.382
14	3.158
13	2.934
12	2.711
11	2.487
10	2.263
9	2.039
8	1.816
7	1.592
6	1.368
5	1.145
4	0.9211
3	0.6974
2	0.4737
1	0.2500

20 ISOVALEURS

Isomach

Boltzmann couplé

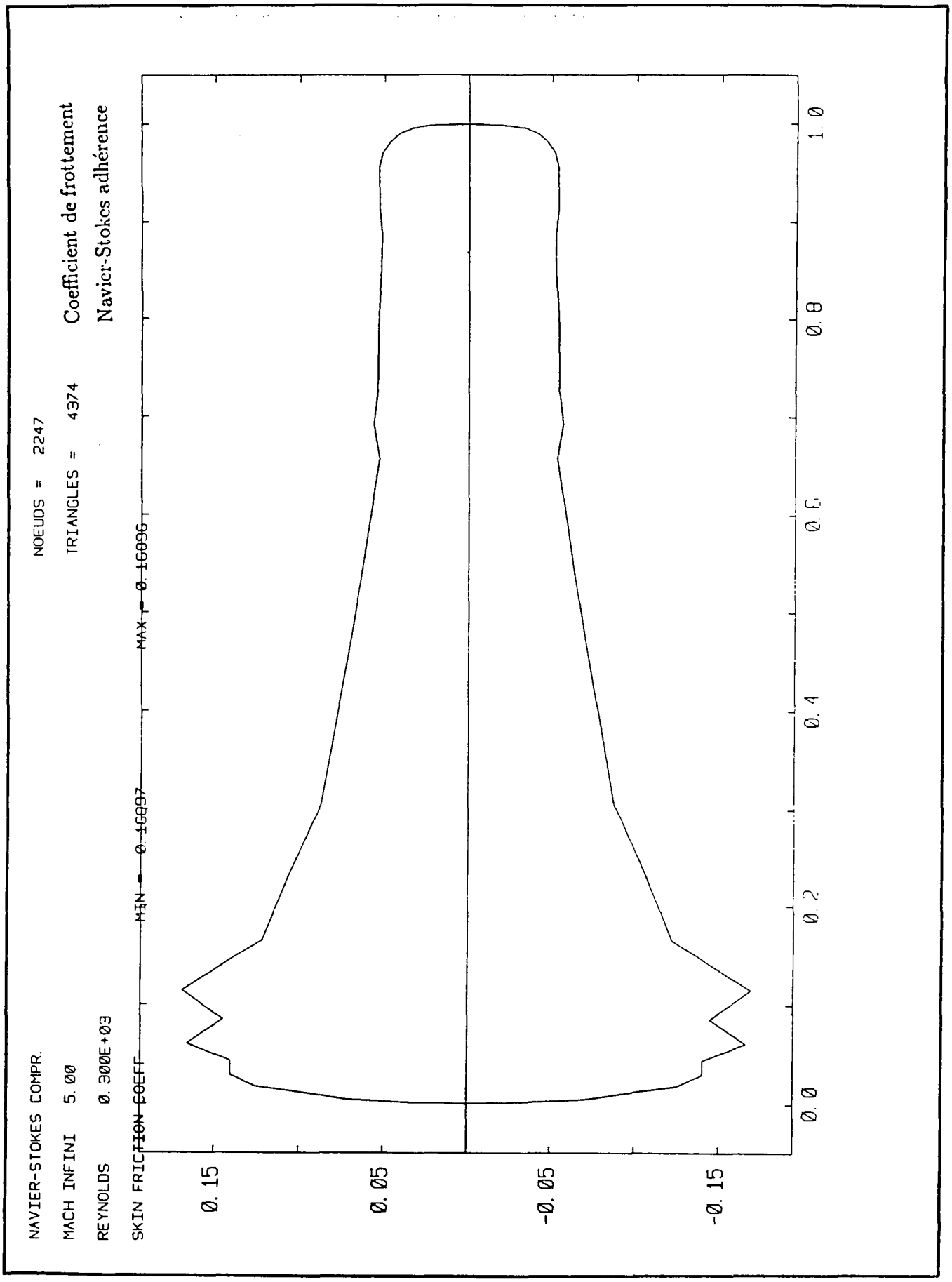
NAVIER-STOKES COMPR.
MACH INFINI 5.00
REYNOLDS 0.300E+03
SKIN FRICTION COEFF MIN = 0.16097 MAX = 0.16096
NOEUDS = 2247
TRIANGLES = 4374
Coefficient de frottement
Navier-Stokes adhérence
0.15
0.05
-0.05
-0.15
0.0
0.2
0.4
0.6
0.8
1.0

Fig. 12.1

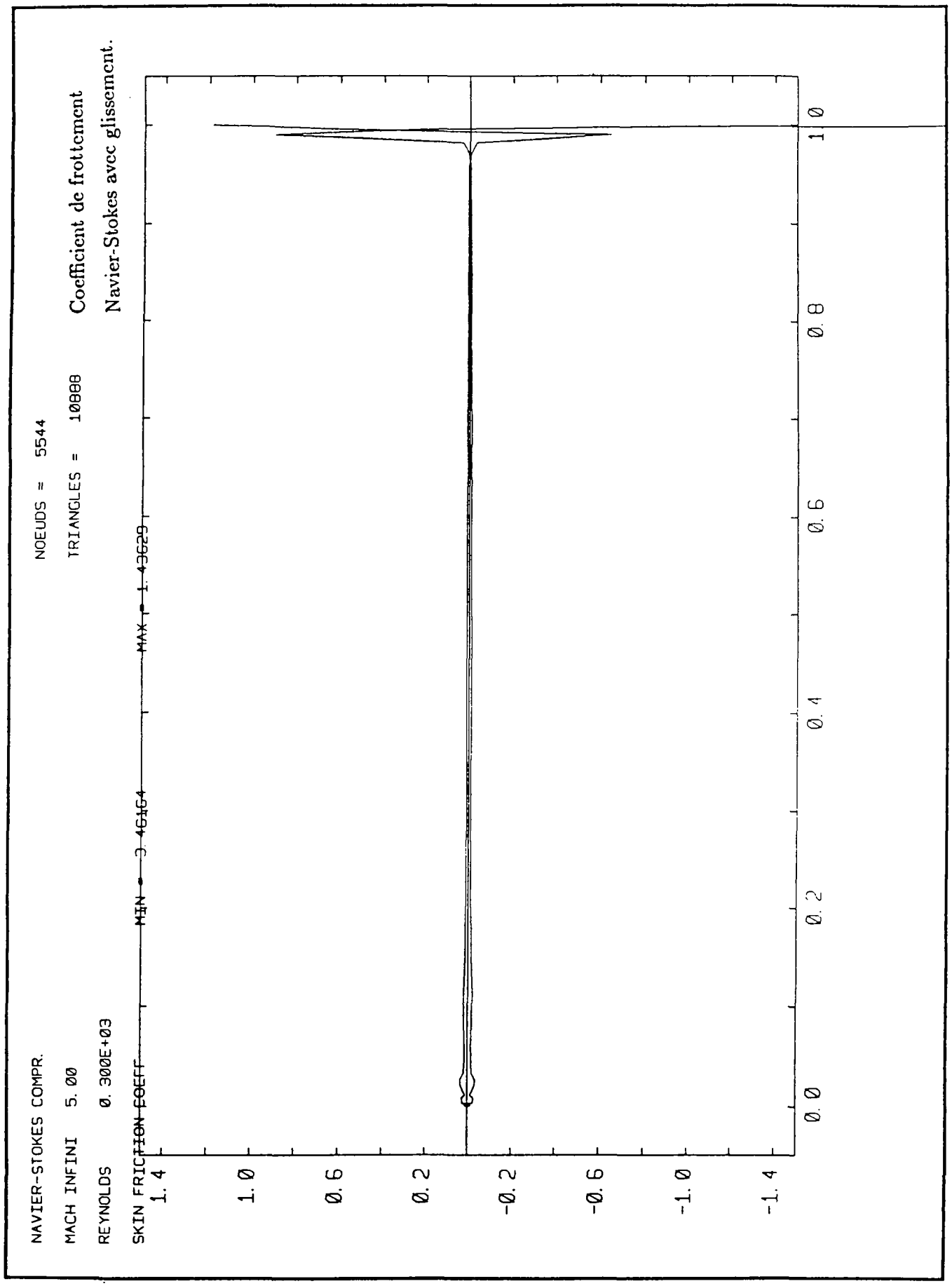
NAVIER-STOKES COMPR.
MACH INFINI 5.00
REYNOLDS 0.300E+03
SKIN FRICTION COEFF
MIN = -3.4644
MAX = 1.4329
NOEUDS = 5544
TRIANGLES = 10888
Coefficient de frottement
Navier-Stokes avec glissement.
1.4
1.0
0.6
0.2
-0.2
-0.6
-1.0
-1.4
0.0
0.2
0.4
0.6
0.8
1.0

Fig. 12.2

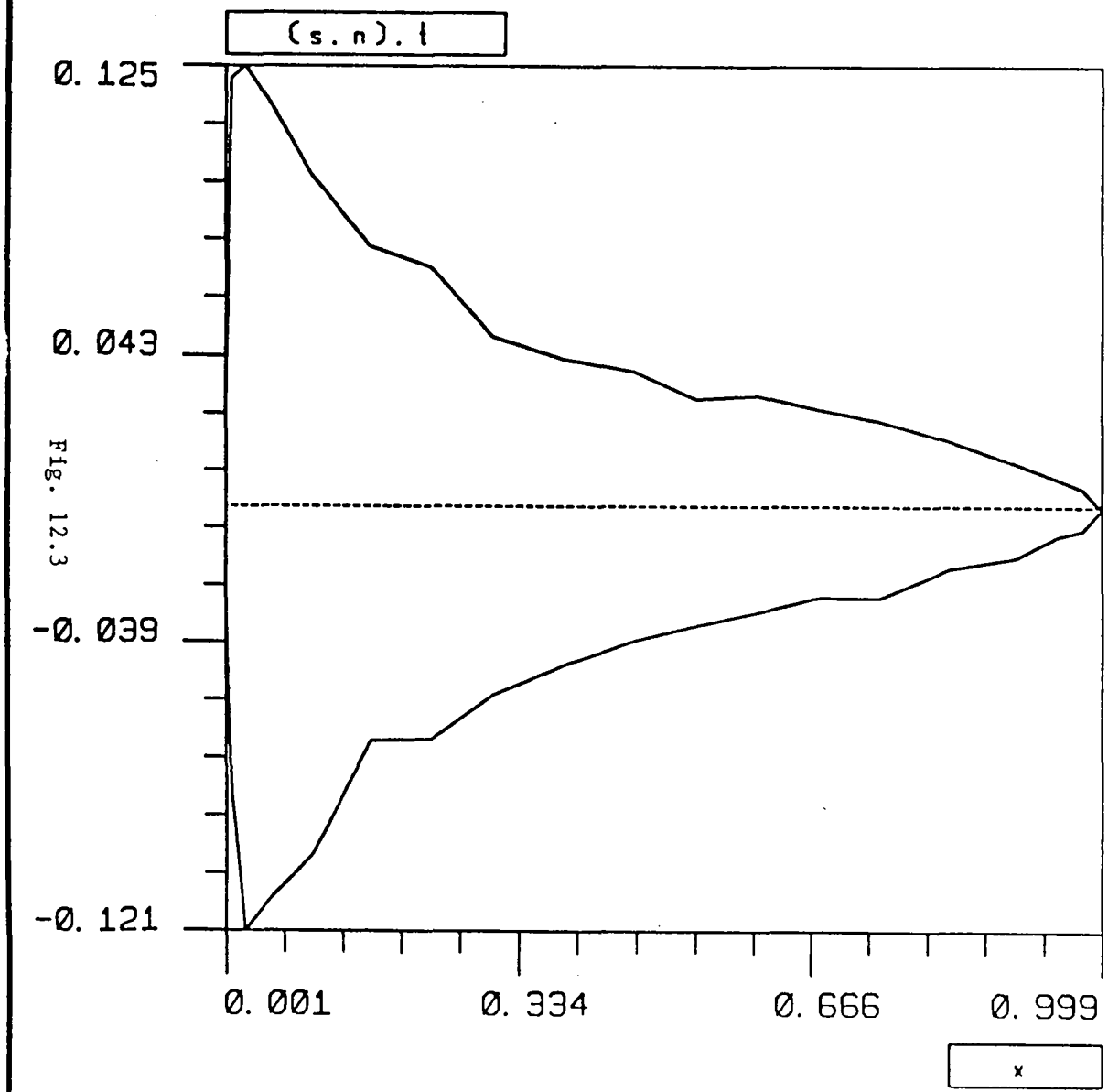

Fig. 12.3

MODULEF

(sigma.n).t

14/12/90

sntns

NOMBRE DE COURBES : 2

EXTREMA EN X :

0.10E-02 1.00

EXTREMA EN Y :

-0.12 0.13

Coefficient de frottement

Boltzmann sur domaine global

TRACE DE COURBES

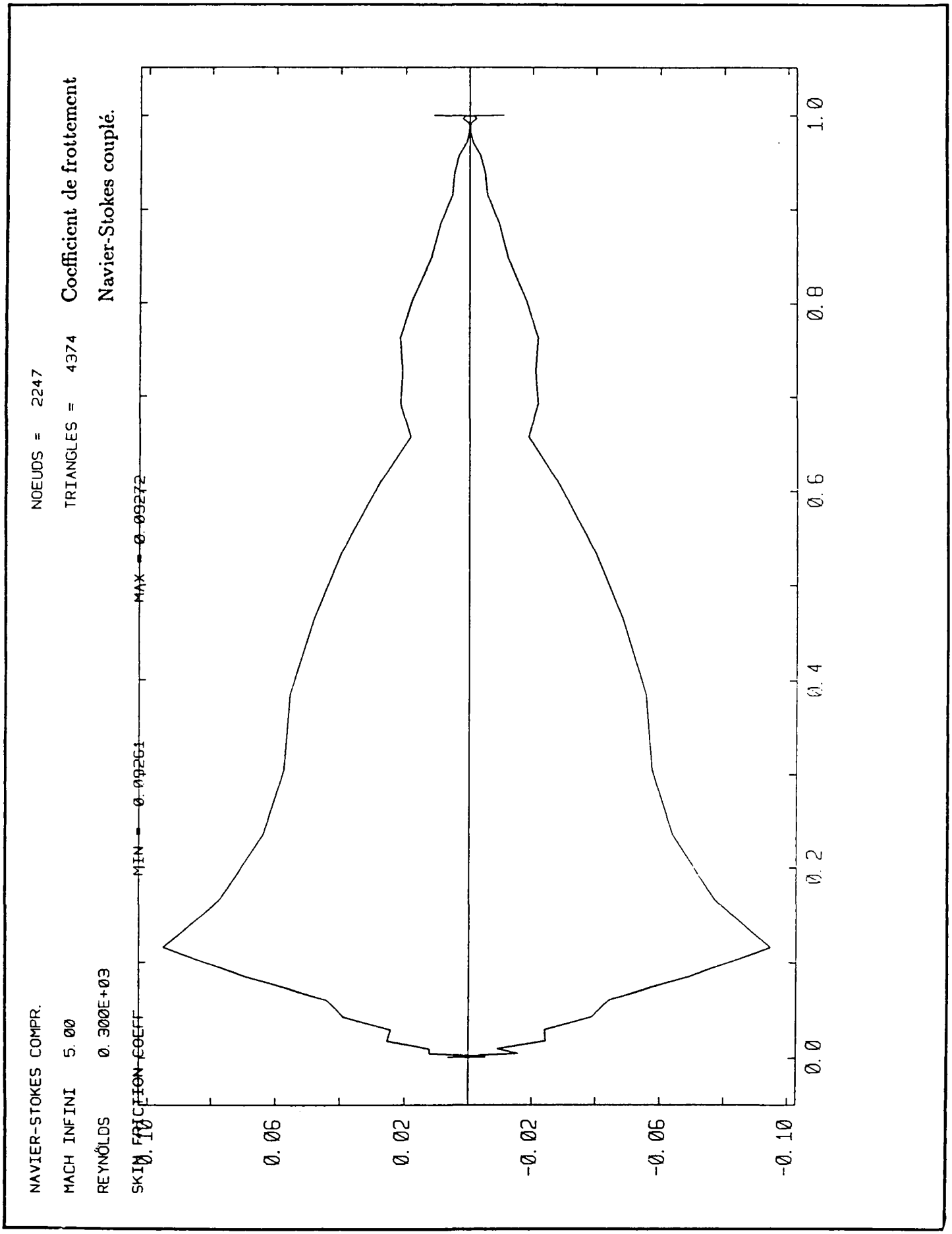
NAVIER-STOKES COMPR.
MACH INFINI 5.00
REYNOLDS 0.300E+03
SKIN FRICTION COEFF
MIN = 0.09261
MAX = 0.09272
NOEUDS = 2247
TRIANGLES = 4374
Coefficient de frottement
Navier-Stokes couplé.
0.10
0.06
0.02
-0.02
-0.06
-0.10
0.0
0.2
0.4
0.6
0.8
1.0

Fig. 12.4

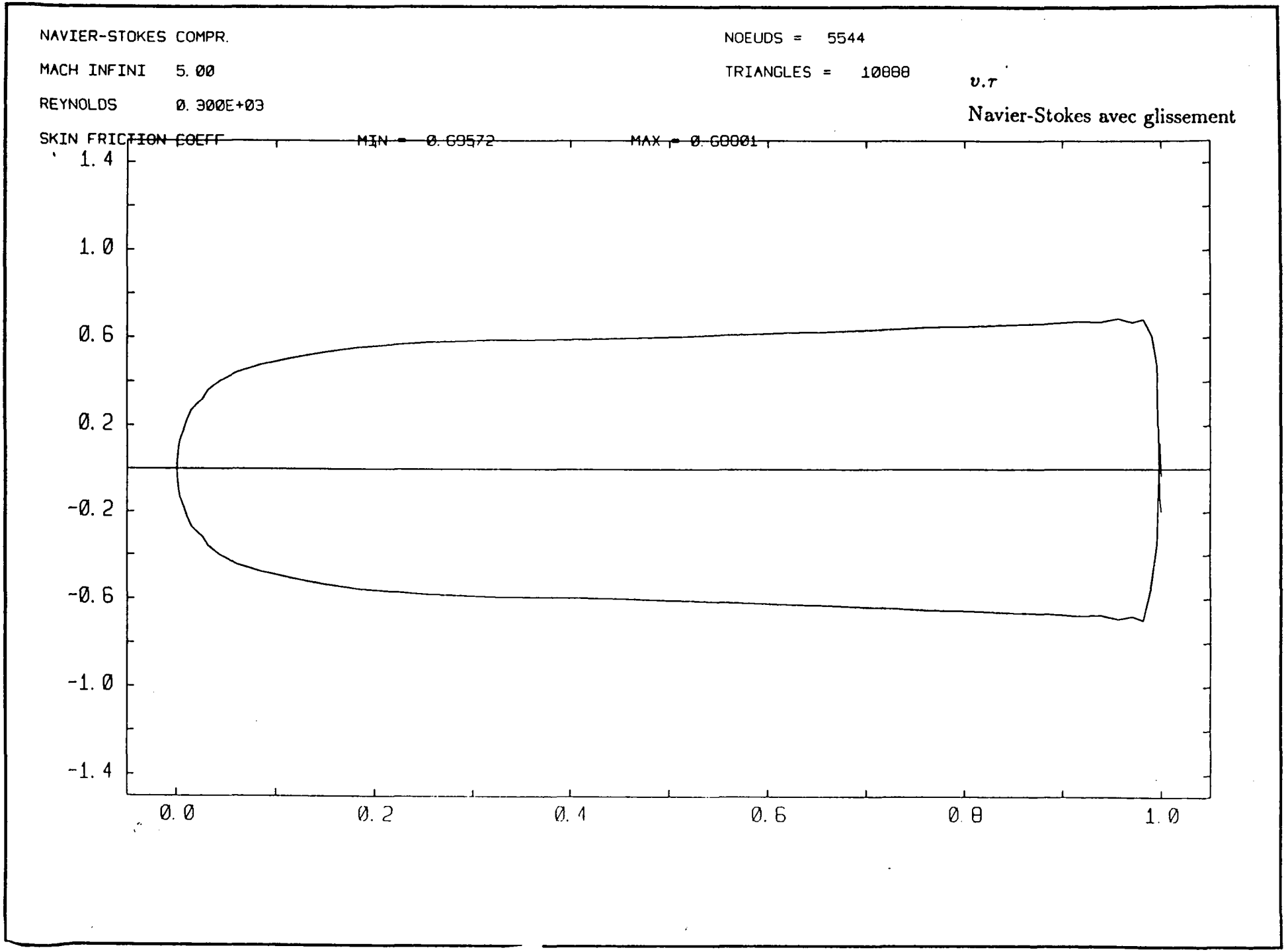

$v.\tau$

Navier-Stokes avec glissement

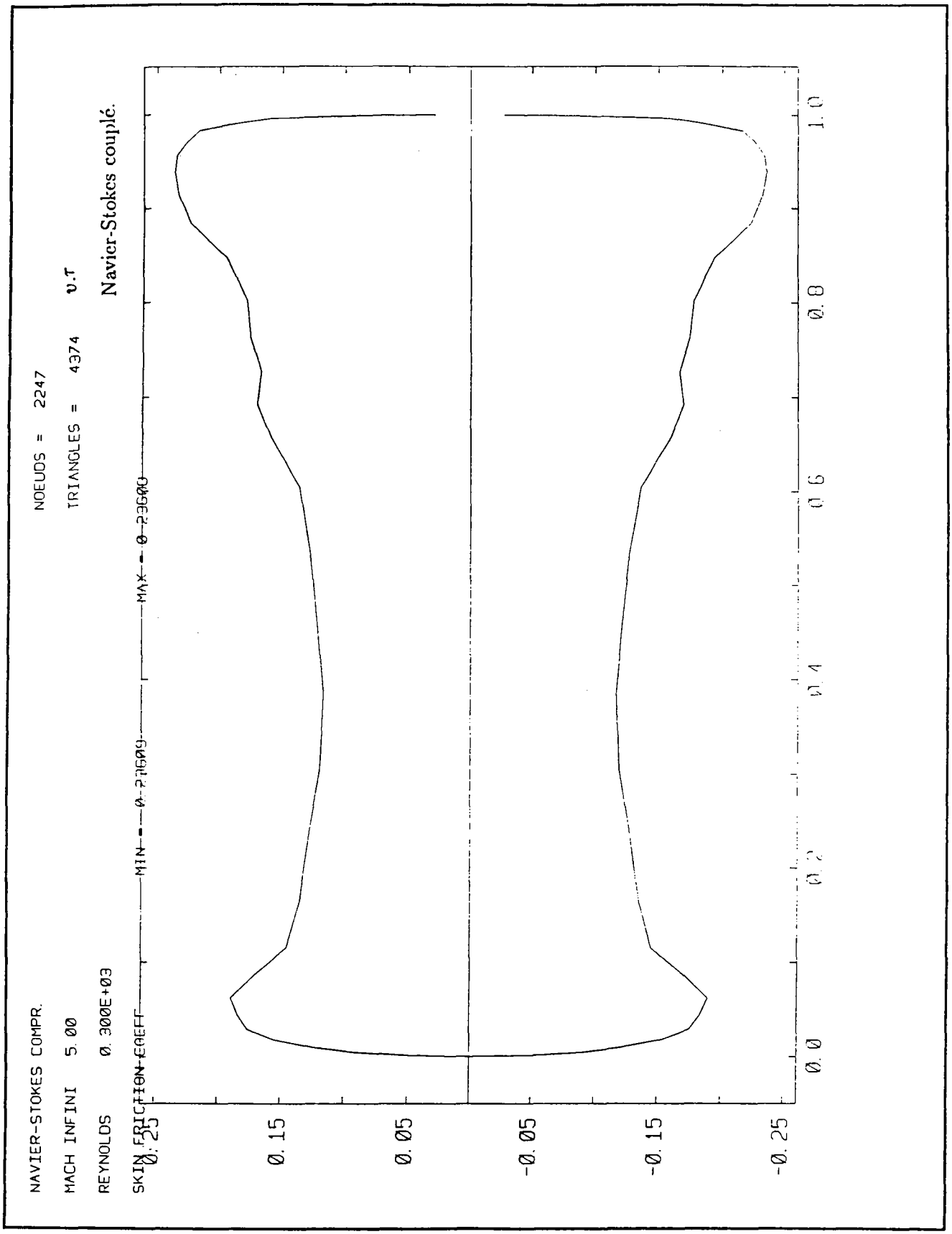

Fig. 13.2

Imprimé en France
par
l'Institut National de Recherche en Informatique et en Automatique.

ISSN 0249 - 6399